

A Simple Solution of Dissolved Ammonia Recovery Process in a Hollow-Fiber Membrane Contactor: Comparison with Experimental and Numerical Results

Eman W. Hassan^{1,#}, O. Chaalal^{2,#} and Md Monwar Hossain^{3,*}

¹National Petroleum Construction Company, P.O. Box 2058, UAE

²Abu Dhabi University, UAE

³Department of Chemical & Petroleum Engineering, United Arab Emirates University, P.O. Box 15551, UAE

Abstract: Ammonia in gaseous form is one of the major pollutants in waters and wastewaters. Of all the processes studied so far for the removal of dissolved ammonia from aqueous solution, hollow fiber membrane contactor-based processes have shown great potential. This method has shown to be effective to substantially reducing ammonia concentration to an acceptable value economically and efficiently. Mathematical analysis is presented in this report for the removal of ammonia dissolved in an aqueous phase to a recovery/stripping solution in a hollow fiber membrane contactor (HFMC). The membrane contactor is considered to consist of the lumen side (allowing aqueous flow) and shell side (allowing the flow of the stripping/recovery solution). An approximate analytical solution is derived for the simplified model that does not include radial diffusion of solutes (only axial mass flux is included). The predicted results of this solution are compared with the experimental data and with the numerical results in the literature over a range of operating conditions. The flow rates of the feed solution covered: 2.01×10^{-9} to 4.7×10^{-6} m³/s, initial concentration: 50 – 800 ppm and pH values of the solution containing ammonia: 8 - 11. The agreement is very good between the profiles of the simplified analytical solution and the earlier published experimental data. In addition, the results obtained by the analytical solution are close to the numerical solution of the complete model over a good range of operating conditions.

Keywords: Ammonia removal, analytical solution, wastewater, hollow-fiber contactor.

1. INTRODUCTION

Several separation techniques have been developed to purify or clean wastewater solutions that are polluted with several pollutants such as, chemical, physical and other types. Ammonia in gaseous form is one of the major pollutants introduced into receiving natural waters by industrial, domestic and agricultural wastewater discharges that scientists are trying to get rid of it using different techniques. This is because the accumulation of this pollutant results in depletion of oxygen due to nitrification and hence harms the water-borne organisms such as fish in addition to its toxicity. For this reason, various techniques have been studied for the removal of dissolved ammonia. They include air stripping, break-point chlorination, chemical precipitation, selective ion exchange, biological nitrification, denitrification, biological nitrification and others [1-4]. These techniques have some drawbacks that let them not to be used. For example, stripping processes are sometimes not suitable for low-concentration wastewater. Also, the disadvantages in break-point chlorination technique are: it requires large treatment volume, the pH is difficult to control and high

chemical costs. Moreover, ion-exchange process requires expensive organic resins and their regeneration in order the overall process to be economic. The biological nitrification and denitrification are slow processes and need large treatment vessels. Because of these disadvantages, membrane processes based on hollow fiber-fiber contactors are considered to be potentially attractive alternative due to its capability in providing large free contact area between the phases where the diffusion of the desired solutes occurs [1-9]. Also, these contactors have the ability to remove low-concentration solutes-especially volatile contaminants- which cannot be achieved by other separation techniques. In addition to that, membrane contactors have lower pressure drop in the gas stripping process due to the tangential flow that results in lower capital cost and ease of operation [1-4, 6, 7]. Among the different types of membrane contactors, hollow fiber membrane contactor with the shell and tube configuration attracts the attention of most of the researchers and scientists due to its advantages such as the capability in setting a dispersion free contact, the velocities of the phases can be selected independently and the absence of flooding, unloading and foaming problems. Another advantage is the indirect contact between the phases that these contactors provide. This indirect contact is because of the chemical concentration gradient between a fluid inside the hollow fiber membrane and a fluid outside a

*Address correspondence to this author at the Department of Chemical & Petroleum Engineering, United Arab Emirates University, P.O. Box 15551, UAE; Tel: +971-3-7135315; Fax: +971-3-7624262;
E-mail: mmonwar@uaeu.ac.ae

#Co-Author E-mail: omar.chaalal@adu.ac.ae; emanh@npcc.ae

hollow fiber membrane. This gradient facilitates the transfer of molecules through the pores of the hollow fiber membrane. The mechanism of separation in these types of contactors depends on the mass transfer between the phases. In this example, ammonia evaporates from the aqueous solution (converted into free gaseous form), diffuses through the membrane pores that is non-wetted by the stripping solution in the other side of the membrane. The main reactions are expressed by the following equations [10, 11]. Eqn. (1) represents the reaction where ammonia in the dissolved form is hydrolysed to ammonium ion depending on pH of the solution (pH less than 8). Eqn. (2) represents how ammonia in the dissolved form is removed from the source phase to another aqueous phase containing sulphuric acid. Other acids and acid containing solutions have been used and suggested for

the stripping [12, 13, 14]. The main purpose of this work is to examine the validity and the applicability of the analytical solutions derived for a simplified model on the experimental and numerical solutions found by others.



2. EXPERIMENTAL (1)

The main chemicals used were analytical grade reagents from Merck and all aqueous solutions were prepared using distilled water. Also, the solutions that contain ammonia were prepared through the addition of measured volumes of ammonium hydroxide to distilled

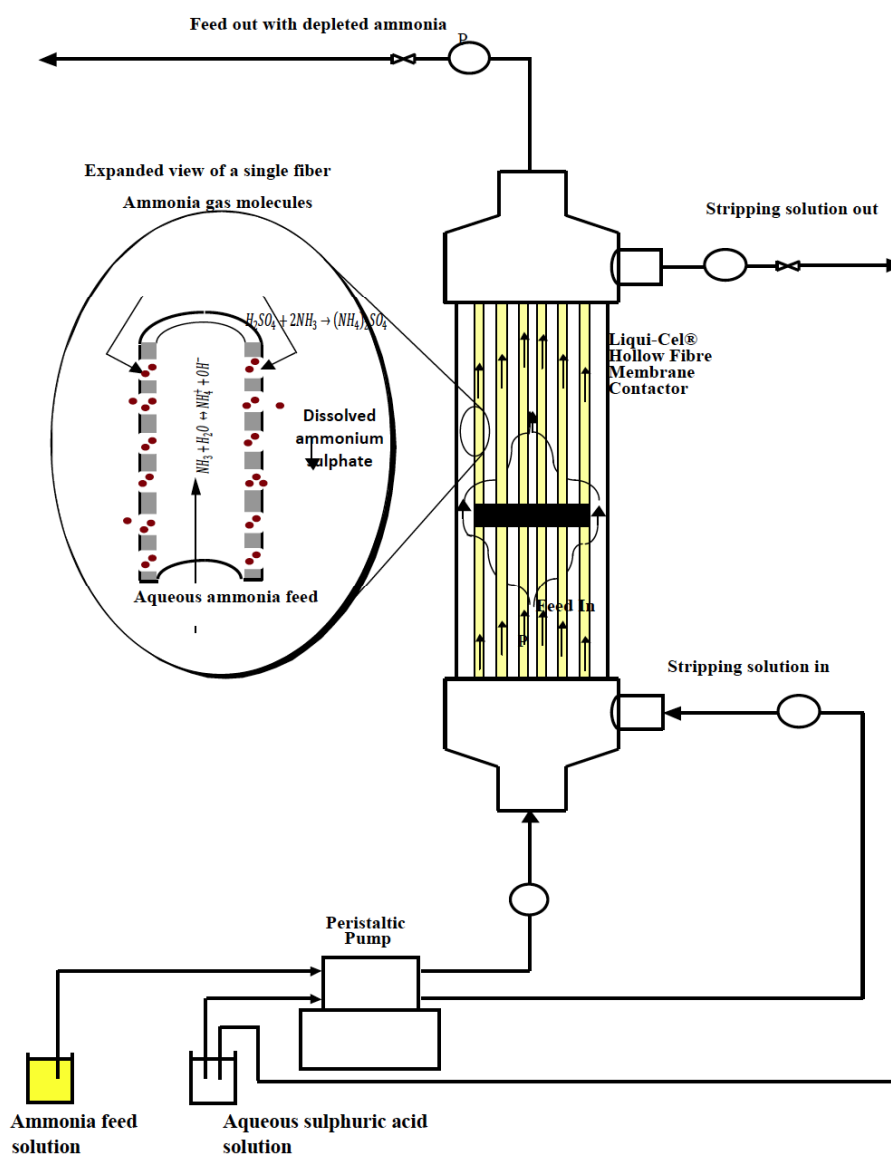


Figure 1: A schematic of the ammonia removal process in a hollow-fiber membrane contactor.

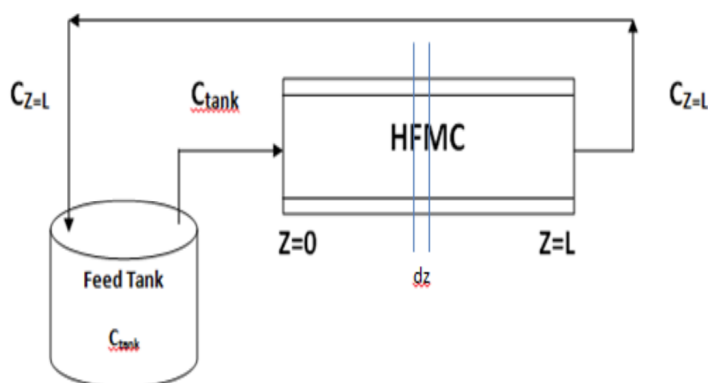


Figure 2: Model domain for the solution: analytical (this work) and numerical simulation¹.

water. Potassium dihydrogen phosphate and dipotassium hydrogen phosphate were used to prepare buffered solutions of aqueous ammonium solutions. On the other hand, the stripping solution was prepared by adding specified volumes of sulfuric acid to distilled water. Then, these solutions (ammonia and stripping solutions) are fed into the HFMC, each in its suitable side (ammonia feed solution in the lumen side and stripping solution in the shell side) between which the transfer occurred through the pores of the membrane as shown in Figure 1. The fibers of the HFMC are hydrophobic polyethylene and are not wetted by any of the aqueous phases. The pores are filled up with the vaporized ammonia (as it is a volatile gas). Because the gas-liquid interface is established on the pore mouth adjacent to the shell side (Figure 1), having the feed solution in the lumen side generates higher contact area between the two phases. The HFMC also works with acid solution on the fiber side and the ammonia feed solution on the shell side (7). Finally, UV-visible Scanning Spectrophotometer was used to measure the ammonia concentration in the samples that were used in the analysis.

Table 1: HFMC Specifications

Parameter	Symbol	Value	Unit
Fiber inner radius	r_{in}	$110^1, 245^4$	μm
Fiber outer radius	r_{out}	$150^1, 365^4$	μm
Fiber porosity	ε	40^1	%
Fiber Tortuosity	$\tau=1/\varepsilon^2$	6.25^1	-
Fiber Length	L	$25^1, 20^2, 30^4$	cm
Number of fibers	N	$6000^1, 10200^2, 75^4$	-
Pore diameter	D	0.03^1	μm
Shell side geometric void fraction	-	0.4^1	-
Effective area	S	1.4^1	m^2
Fiber Volume	V_f	200	ml
Shell Volume	V_s	400	ml
Feed Volume	V_F	$5000^1, 1500^4$	ml

3. MASS TRANSFER MODEL

3.1. Process Description

Figure 1 shows the process steps occurring in the hollow fiber membrane contactor (HFMC). In this contactor, the stripping solution flows in the shell side, whereas the aqueous feed solution is fed to the lumen side. By contacting the two solutions in the membrane contactor, ammonia in gaseous form is transferred by diffusion and convection mechanisms from the feed bulk towards the feed-membrane interfaces through the non-wetted (gaseous) pores of the membrane. The characteristics of the HFMC and the experimental operating conditions in getting the solutions of the model equations are shown in Tables 1 and 2, respectively.

3.2. Equations of the Mathematical Model

As mentioned before, stripping/recovery solution flows in the shell side of the HFMC, however aqueous feed solution is fed from the source of the solution (reservoir or tank @ $z=0$) to the lumen side of the

Table 2: Experimental Operating Parameters

Parameter	Rezazazemi et al. (2012) ¹				Mandowara (2011) ²	Tan (2006) ⁴
	Run#1	Run#2	Run#3	Run#4		
C _o (ppm)	50	200	400	800	227.97	126
Q _L (m ³ /s)	2.014*10 ⁻⁹	8.093*10 ⁻⁹	4.027*10 ⁻⁹	6.079*10 ⁻⁹	4.7*10 ⁻⁶	6.597*10 ⁻⁸
pH	8	10	11	9	10.5	10
P(atm)	1	1	1	1	1	1
T(K)	293	293	293	293	298	298
k _o (x10 ⁵) (m/s)	0.12	1.32	1.31	0.69	1.44	1.455

contactor as shown in Figure 2¹. Then, ammonia flows through the lumen side, vaporized into the pores, diffuses to the shell side, reacts with sulphuric acid on the shell side (thus ammonia is removed) and transported by diffusion on the bulk solution. These mechanisms are based on the following assumptions [1, 2, 4]:

- Isothermal process
- Fully developed parabolic profile (for complete model) in the lumen side
- Plug flow profile (for the simplified model) in the lumen side
- There is no reaction zone (the reaction of ammonia with the stripping solution is very fast (instantaneous)).
- No pore blockages and pores are filled with air (non-wetting)
- Feed, extract and tank volumes are large compared to that of the hollow fiber module

- Flow rates of ammonia solution is constant
- Feed tank operates at the perfect mixing mode
- The solution in the tank has been recycled

The model equations and their solutions are listed in Table 3.

Equations on the lumen side [3, 8]

- Complete model:

$$\frac{\partial C}{\partial t} + D_{NH_3-lumen} \left[\frac{\partial^2 C}{\partial r^2} + \frac{1}{r} \frac{\partial C}{\partial r} + \frac{\partial^2 C}{\partial z^2} \right] = v_{z-lumen} \frac{\partial C}{\partial z} \quad (3)$$

- Simplified model (This work)

$$\frac{dC}{dz} = \frac{k_o \pi d_i}{Q_L} (mC_G - C) \quad (4)$$

Where C is the dissolved concentration of ammonia in the liquid phase (mol/m³), $D_{NH_3-lumen}$ is the diffusivity of ammonia in the lumen side $\left(\frac{m^2}{s}\right)$, r is the radial distance (m), z is the axial distance (m), axial velocity

Table 3: Model Equations and their Solutions

Mass Balance	Main Equation	Boundary conditions	Solution*
Tank	$\frac{dC_t}{dt} = \left(\frac{Q}{V}\right) * (C_L - C_t)$	@ t=0, C _t = C _o	$C_{tank} = C_o e^{\left(\frac{Q}{V}\right)t * \left(\frac{V_f}{V_s} - \frac{V_f - (1 + \frac{V_f}{V_s})}{1 + \frac{V_f}{V_s}}\right) e^{-\left(1 + \frac{V_f}{V_s}\right) \left(\frac{k_o \pi d_i}{Q_L}\right)L}}$
Lumen (C _L)	$\frac{dC}{dz} = \frac{k_o \pi d}{Q_L} (mC_G - C)$	@ z=0, C = C _t @ z=L, C = C _L	$C_z = \left(\frac{C_{tank}}{1 + \frac{V_f}{V_s}}\right) * \left(\frac{V_f}{V_s}\right) - \left(\frac{V_f}{V_s} - \left(1 + \frac{V_f}{V_s}\right)\right) e^{-\left(1 + \frac{V_f}{V_s}\right) \left(\frac{k_o \pi d_i}{Q_L}\right)L}$ $C_L = mC_G (1 - e^{-\left(\frac{k_o \pi d_i}{Q_L}\right)L})$

in the contactor, k_o is the overall mass transfer coefficient (m/s), d_i is the lumen inner diameter (m), Q_L is the liquid flow rate in one fiber (m^3/s), m is the distribution coefficient (-), C_G is the ammonia concentration in gaseous form (mol/m^3).

3.3. Mass Balance in the Ammonia Tank

The mass balance equation for ammonia in the tank is derived under the assumption of uniform mixing and it is as follows [9]:

$$\frac{dC_t}{dt} = \left(\frac{Q}{V_F}\right) * (C_L - C_t) \quad (5)$$

Where Q is the total volumetric flow rate (m^3/s), V_F is the volume of the feed solution (m^3), t is the time (s), and C_t is ammonia concentration, (mol/m^3) and C_L is the ammonia concentration at the outlet of the contactor which is the inlet of the feed tank as shown in Figure 2. The boundary and the initial conditions are the following:

- Boundary condition:

$$@ z = 0, C = C_{\text{tank}} (C_t) \quad (6)$$

- Initial condition

$$@ t = 0, C_t = C_o \quad (7)$$

3.4. Analytical Solutions of the Model Equations

For the analytical solutions of the equations, mC_G in Eqn. (4) is calculated, from the material balance between the flowing masses. That is the moles of ammonia transferred and diffused into the shell side ($mC_G V_S$) equals to the difference in the number of moles of ammonia between the tank ($V_f C_{\text{tank}}$) and lumen ($V_f C$) sides. With this mass balance (Eqn. (7)), Eqn. (4) simplifies to Eqn. (8)

$$mC_G = \frac{V_f}{V_S} (C_t - C) \quad (7)$$

$$\frac{dC}{dz} = R * (FC_t - EC) \quad (8)$$

$$\text{-Where } R : \frac{k_o \pi d_i}{Q_L}, F : \frac{V_f}{V_S}, E : 1 + \frac{V_f}{V_S} \quad (9)$$

and $Q_L = A_{\text{cross fiber}} * U_{\text{avg}} = \pi r_i^2 * U_{\text{avg}}$ (For plug flow, since the radial effect on concentration has not been taken into consideration, so the velocity equals the average velocity not 2*average velocity). The solution

to Eqn. (8) is derived by integration and is given in Eqn. (10):

$$C = \frac{C_t}{E} (F - (F - E)e^{-ERZ}) \quad (10)$$

$$C_{z=L} = \frac{C_L}{E} (F - (F - E)e^{-ERL}) \quad (11)$$

Mass balance in the tank:

The solution involves substitution of Eqn. (11) at $z = L$ in Eqn. (3) and integration of the resulting equation, Eqn. (12). The final form of the solution is Eqn. (13)

$$\frac{dC_t}{dt} = \left(\frac{Q}{V_F}\right) * \left(\frac{C_t}{E} (F - (F - E)e^{-ERL}) - C_t\right) \quad (12)$$

$$C_t = C_o e^{\left(\frac{Q}{V_F}\right) t \left(\frac{F - (F - E)}{E} e^{-ERZ} - 1\right)} \quad (13)$$

The details of this procedure are discussed in the appendix.

4. RESULTS & DISCUSSION

In Figure 3 the ratio of the normalized ammonia tank concentration (its ratio to that of the initial concentration value) versus time is shown. The operating variables are: initial ammonia concentration range of 126-594 ppm, constant feed velocity of 0.35 m/s and ammonia solution pH of 10 (4). The ammonia concentration in the tank (experimental) decreased exponentially as the contact time increased and attained 20% of the initial value within 100 minutes for all the concentrations tested in the experiment. This effect is similar to those reported earlier in Figures 5 of reference 1 and are redrawn as Figure 4 to show the similarity. The analytical solution (dotted line) derived in this paper, is able to predict the experimental data (dot) and almost as good as the numerical simulation (solid line) for the range of ammonia concentration considered (Figure 3).

Figure 5 shows the effect of feed velocity in the range 0.059 – 0.825 m/s on the normalized ammonia tank concentration at constant ammonia concentration of 120 ppm and at solution pH of 10 (4). With the increase in the feed velocity up to a value of 0.589 m/s, the ammonia tank concentration decreased resulting in more removal of ammonia in the process. This is due to the reduction of the mass transfer resistance on the aqueous feed side, as the velocity is increased allowing

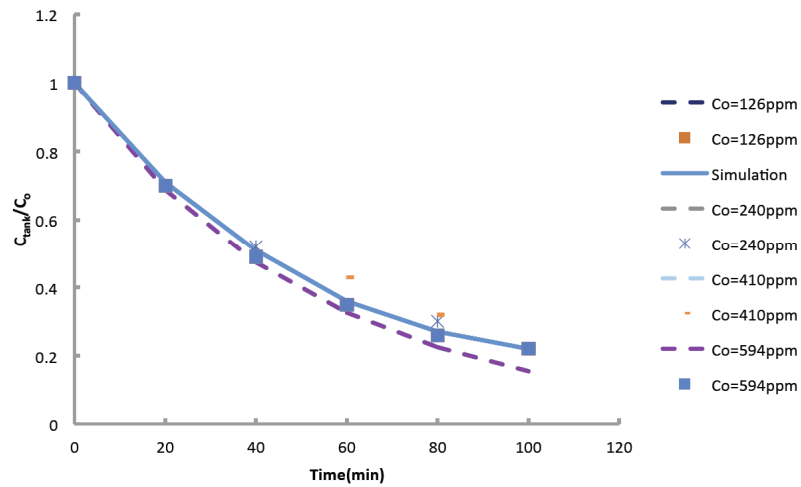
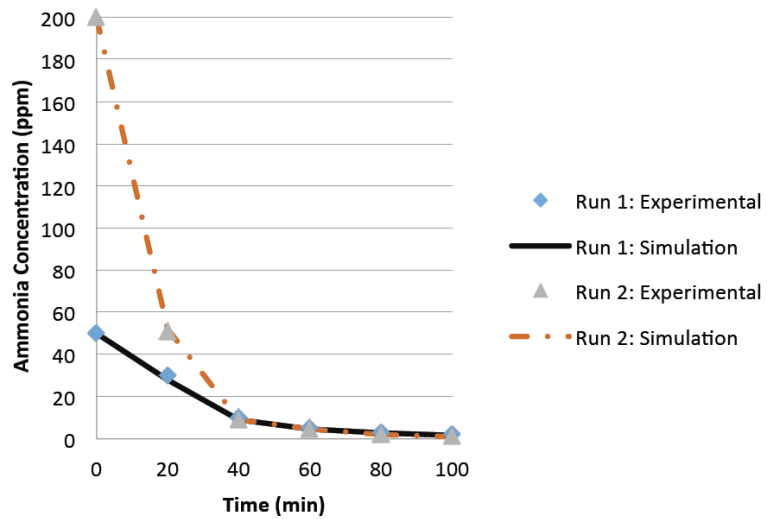
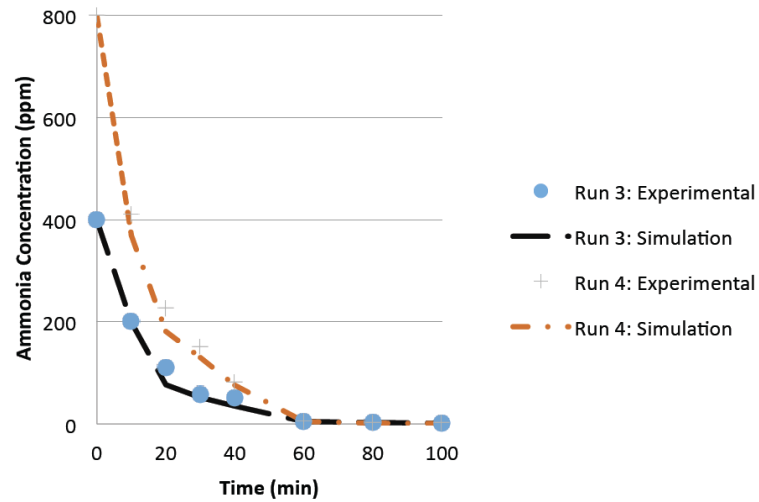


Figure 3: Ammonia tank concentration (dimensionless with respect to initial ammonia concentration) vs. time (min): Comparison between simulation (solid line), experimental data (dots)¹ and results of the analytical solution (dashed line) for the effect of initial ammonia concentration.



a



b

Figure 4: Ammonia tank concentration (dimensionless with respect to initial ammonia concentration) vs. time (min): Comparison between experimental data (dots)², and the simulated results (solid line), (redrawn from Figure 5a and 5b of reference [1]).

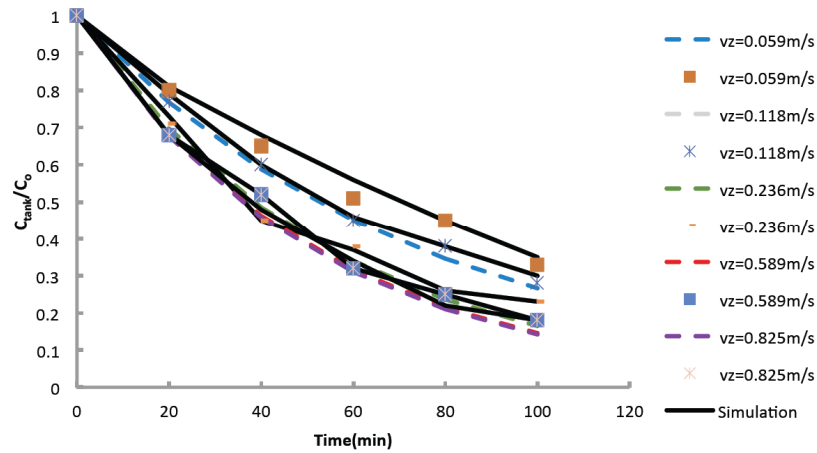


Figure 5: Ammonia tank concentration (dimensionless with respect to initial ammonia concentration) vs. time (min), Comparison between the simulation (solid line) experimental (dots)⁴ and results of the analytical solution (dashed line) for the effect of feed velocity.

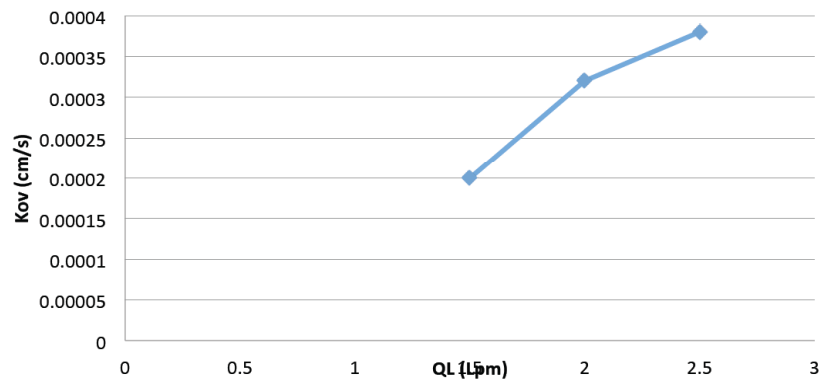


Figure 6: The effect of the feed flow rate on the overall mass transfer coefficient (redrawn from Figure 7 of reference [11]).

more decrease in the tank concentration. Beyond this feed velocity (i.e. greater than 0.589 m/s) the other resistances (possibly membrane mass transfer that is the same for all flow rates) dominates the overall process and the decrease in ammonia removal is minimal (i.e. the profile of ammonia tends to level off with time). The increase in the overall mass transfer coefficient with the flow rate was determined in the literature (Figure 7 of reference 11) and the results are redrawn as in Figure 6. In all the calculations, the predicted results of the analytical solution is similar to those of the experimental data and very close to those obtained by the simulation of the full mathematical model.

Figure 7 shows the variation in experimental ammonia concentration (dimensionless ratio with respect to the initial feed concentration) as function of a combination of feed flow rate and initial ammonia concentration. The results of the analytical solution is shown and they follow closely the experimental data over the entire range of conditions. The experimental

conditions used in the analytical calculations are the same as in the literature (2) and these are listed in Table 2. As can be seen in Figure 7 that the predicted results of the analytical are very close considering a good range of conditions covered in the calculations. Therefore, the simplified model solution can be used to calculate the predicted tank ammonia concentration over a good range of concentration and feed velocity.

Figure 8 shows the effect of pH on the removal fraction of ammonia ($\beta=1-C_{\text{tank}}/C_0$) [2], and its comparison with the results of this work at $t = 4800\text{s}$ (nearly the end of the process). Although the values of both results are not exactly the same, the overall trend is similar. As the ammonia solution pH increased, its removal increased, reached a maximum value (close to 95%) and remained constant for ammonia solution value up to pH 12. This is because ammonia presents in gaseous form only at higher values of pH (greater than pH 10) and this condition allows more amount of dissolved ammonia to be removed from the aqueous solution. At lower pH, the other fraction of total

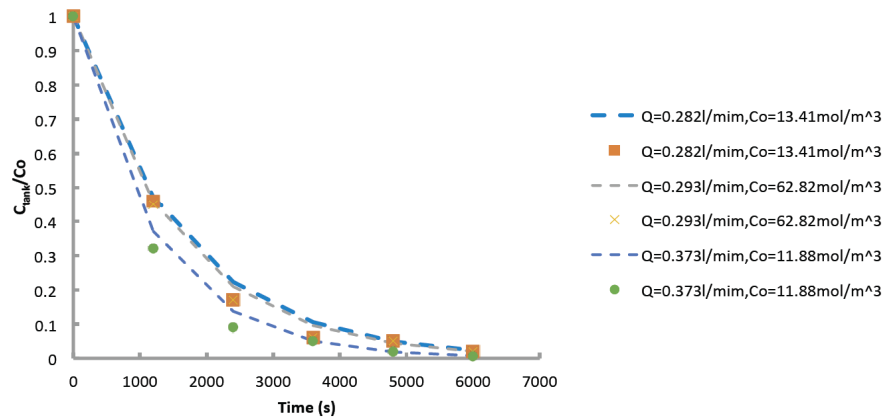


Figure 7: Ammonia tank concentration (dimensionless with respect to initial ammonia concentration) vs. time (s), for three variables: feed solution pH, initial ammonia concentration and feed flow rate; Comparison between the experimental data (dots)⁴ and results of the analytical solution (dashed line).

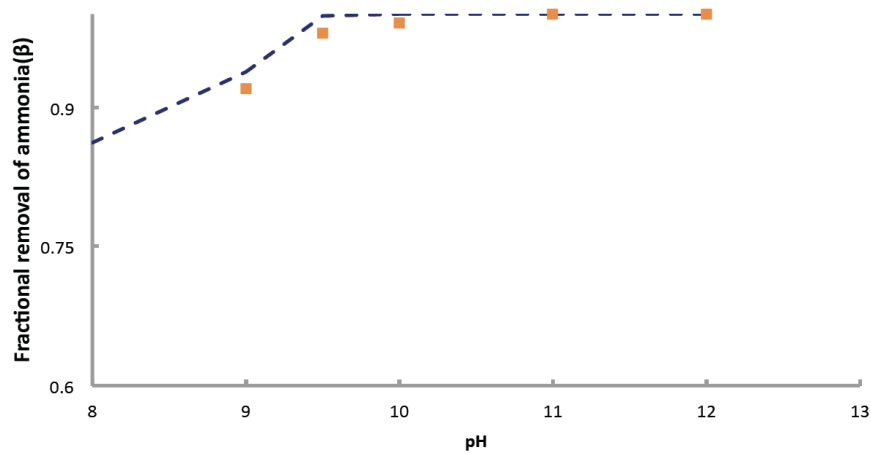


Figure 8: Fractional removal of ammonia vs. pH, the analytical solution results (dashed), experimental results (dotted)² at $t=4800\text{s}$.

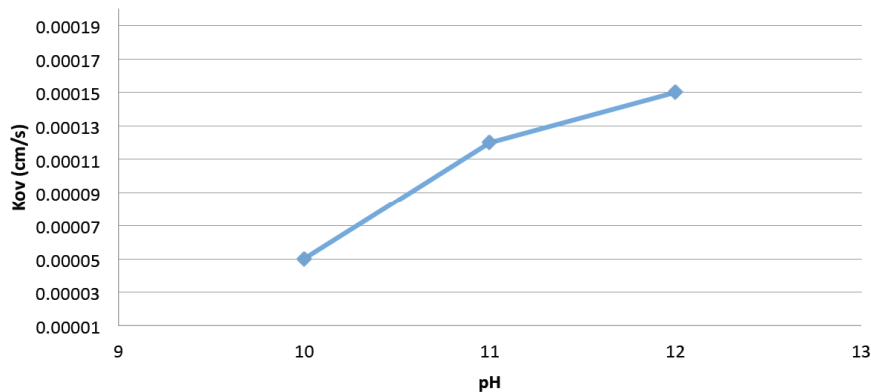


Figure 9: The effect of feed pH on the overall mass transfer coefficient (redrawn from Figure 3 of reference [11]).

concentration, NH_4^+ , dominates which is nonvolatile and does not diffuse through the pores of the membrane. In reference 11 (Figure 3), the overall mass transfer coefficient was determined and shown to increase with the ammonia solution pH in the range 10-12. This is redrawn in Figure 9 to explain higher ammonia removal with the increase of pH (Figure 7).

5. CONCLUSIONS

The analytical solutions of the simplified model for ammonia concentrations in the hollow fiber membrane contactor and in the reservoir tank are presented. The solutions depend on the operating conditions (feed flow rate, solution volume and its pH) and dimensions of the

hollow-fiber contactor. The predictions of the analytically derived equations follow closely the experimental data, i.e. the percentage ammonia removal that (i) increased with solution pH (in the range 8- 12), (ii) increased with the feed velocity (0.059 – 0.825 m/s) and (iii) slightly affected by the initial dissolved ammonia concentration (50 – 800 ppm). These predictions are similar to those of the simulation results of the complete model for the ammonia removal process examined in hollow-fiber membrane contactors with various number of fibers 75, 6000 and 10,200.

ACKNOWLEDGEMENT

The authors would like to thank UAE University, Al Ain, United Arab Emirates for overall support to compile this work.

NOMENCLATURE

- A = cross section of tube, m²
 C = Ammonia concentration in the lumen side, mol/m³
 C_L = ammonia concentration in the lumen side at the exit, mol/m³
 C₀ = Initial ammonia concentration, mol/m³
 d_i = inner diameter of the fiber, μm
 D = pore diameter, μm
 E = 1+ V_f/V_s
 F = V_f/V_s
 k_o = overall mass transfer coefficient, m/s
 m = the distribution coefficient (-)
 P = Pressure, atm
 Q_L = volumetric flow rate in the tube, m³/s
 R = k_oπd_i/Q_L(1/m)
 t = time, s
 V_F = the feed volume, ml
 z = axial coordinate, m

Greek Symbols

- ε = Fiber porosity
 τ = fiber tortuosity

APPENDIX A

The mass balance equation for ammonia in the tank is derived under the assumption of uniform mixing and it is as follows:

$$\frac{dC_t}{dt} = \left(\frac{Q}{V_F}\right) * (C_L - C_t) \quad (A1)^9$$

Where Q is the volumetric flow rate, m³/s, t is the time, s, and C is ammonia concentration, mol/m³. C_L is the ammonia concentration at the outlet of the contactor which is the inlet of the feed tank as shown in Figure 2

Analytical Solutions of the Model Equations

In order to get the analytical solutions of the equations, the following steps have been used with the previous mentioned assumptions and following boundary conditions as under:

*lumen Side:

- Boundary Conditions:

$$@z=0, C=C_{\text{tank}}^1 \quad (A2)$$

$$\frac{dC}{dz} = \frac{k_o \pi d_i}{Q_L} (mC_G - C) \quad (A3)$$

mC_G is obtained from the following material balance which indicates that the moles of ammonia transferred and diffused into the shell side (mC_GV_S) equals to the difference in the number of moles of ammonia between the tank (V_fC_t) and lumen (V_fC) sides :

$$mC_G = \frac{V_f}{V_s} (C_t - C) \quad (A4)$$

$$\frac{dC}{dz} = \frac{k_o \pi d_i}{Q_L} \left(\frac{V_f}{V_s} (C_t - C) - C \right) \quad (A5)$$

$$\frac{dC}{dz} = \frac{k_o \pi d_i}{Q_L} \left(\frac{V_f}{V_s} C_t - C \left(1 + \frac{V_f}{V_s} \right) \right) \quad (A6)$$

$$\frac{dC}{dz} = R * (FC_t - EC) \quad (A7)$$

$$\frac{dC}{FC_t - EC} = Rdz \quad (A8)$$

$$\int \frac{dC}{FC_t - EC} = \int Rdz \quad (A9)$$

$$-\frac{1}{E} \ln(FC_t - EC) = RZ + C_1 \quad (A10)$$

$$@z=0, C=C_t \quad (A11)$$

$$C_1 = -\frac{1}{E} \ln(C_t(F - E)) \quad (A12)$$

$$-\frac{1}{E} \ln(FC_t - EC) = RZ - \frac{1}{E} \ln(C_t(F - E)) \quad (A13)$$

$$\ln(FC_t - EC) = -ERZ + \ln(C_t(F - E)) \quad (A14)$$

$$EC = FC_t - C_t(F - E)e^{-ERZ} \quad (A15)$$

$$C = \frac{F}{E} C_t - \frac{1}{E} C_t(F - E)e^{-ERZ} \quad (A16)$$

$$C = \frac{C_t}{E} (F - (F - E)e^{-ERZ}) \quad (A17)$$

$$C_{z=L} = \frac{C_t}{E} (F - (F - E)e^{-ERL}) \quad (A18)$$

Mass balance in the tank:

- Boundary Conditions:

$$@ t=0, C_t = C_o \quad (A19)$$

- Solution Steps:

$$\frac{dC_t}{dt} = \left(\frac{Q}{V_F}\right) * (C_L - C_t) \quad (A20)$$

$$\frac{dC_t}{dt} = \left(\frac{Q}{V_F}\right) * \left(\frac{C_t}{E} (F - (F - E)e^{-ERL}) - C_t\right) \quad (A21)$$

$$\frac{dC_t}{dt} = \left(\frac{Q}{V_F}\right) * \left(\frac{C_t}{E} F - \frac{C_t}{E} (F - E)e^{-ERL} - C_t\right) \quad (A22)$$

$$\frac{dC_t}{dt} = \left(\frac{Q}{V_F}\right) * C_t \left(\frac{F}{E} - \frac{(F - E)}{E} e^{-ERL} - 1\right) \quad (A23)$$

$$\frac{dC_t}{C_t} = \left(\frac{Q}{V_F}\right) \left(\frac{F}{E} - \frac{(F - E)}{E} e^{-ERL} - 1\right) dt \quad (A24)$$

$$\int_{C_o}^{C_t} \frac{dC_t}{C_t} = \int_0^t \left(\frac{Q}{V_F}\right) \left(\frac{F}{E} - \frac{(F - E)}{E} e^{-ERL} - 1\right) dt \quad (A25)$$

$$\ln C_t - \ln C_o = \left(\frac{Q}{V_F}\right) t \left(\frac{F}{E} - \frac{(F - E)}{E} e^{-ERL} - 1\right) \quad (A26)$$

$$\ln \left(\frac{C_t}{C_o}\right) = \left(\frac{Q}{V_F}\right) t \left(\frac{F}{E} - \frac{(F - E)}{E} e^{-ERL} - 1\right) \quad (A27)$$

$$C_t = C_o e^{\left(\frac{Q}{V_F}\right) t \left(\frac{F}{E} - \frac{(F - E)}{E} e^{-ERL} - 1\right)} \quad (A28)$$

REFERENCES

- [1] Rezakazemi M, Shirazian S, Ashrafizadeh S. Simulation of ammonia removal from industrial wastewater streams by means of hollow-fiber membrane contactor. *Desalination* 2012; 285: 383-392. <https://doi.org/10.1016/j.desal.2011.10.030>
- [2] Mandowara A, Bhattacharya P. Simulation studies of ammonia removal from water in a membrane contactor under liquid-liquid extraction mode. *J Environ Manage* 2011; 92: 121-130. <https://doi.org/10.1016/j.jenvman.2010.08.015>
- [3] Mandowara A, Bhattacharya P. Membrane contactor as degasser operated under vacuum for ammonia removal from water: A numerical simulation of mass transfer under laminar flow conditions. *Comp Chem Eng* 2009; 33: 1123-1131. <https://doi.org/10.1016/j.compchemeng.2008.12.005>
- [4] Tan X, Tan SP, Teo WK, Li K. Polyvinylidene fluoride (PVDF) hollow fiber membranes for ammonia removal from water. *J Membr Sci* 2006; 271: 59-68. <https://doi.org/10.1016/j.memsci.2005.06.057>
- [5] Kunz A, Mukhtar S. Hydrophobic membrane technology for ammonia extraction from wastewaters. *Eng Agric* 2016; 36: 1-11. <https://doi.org/10.1590/1809-4430-Eng.Agric.v36n2p377-386/2016>
- [6] Ashrafizadeh SN, Khorasani Z. Ammonia removal from aqueous solutions using hollow-fiber membrane contactors. *Chem Eng J* 2010; 162: 242-249. <https://doi.org/10.1016/j.cej.2010.05.036>
- [7] Hasanoglu A, Romero J, Perez B, Plaza A. Ammonia removal from wastewater streams through membrane contactors: Experimental and theoretical analysis of operation parameters and configuration. *Chem Eng J* 2010; 160: 530-537. <https://doi.org/10.1016/j.cej.2010.03.064>
- [8] Licon E, Reig M, Villanova P, Valderrama C. Ammonia removal by liquid-liquid membrane contactor under closed loop regime, Excerpt from the Proceedings of the 2012 COMSOL Conference, Milan, Italy.
- [9] Rawat A, Agrahari GK, Pandey N, Bhattacharya PK. Mathematical analysis of removal of dissolved acidic gases from aqueous stream using membrane contactor. *Intl J Chem Eng Appl* 2013; 4: 290-294. <https://doi.org/10.7763/IJCEA.2013.V4.312>
- [10] Kartohardjono S, Damaiati GM, Rama CT. Effects of absorbents on ammonia removal from wastewater through hollow fiber membrane contactor. *J Environ Sci Technol* 2015; 8: 225-231. <https://doi.org/10.3923/jest.2015.225.231>
- [11] Kartohardjono S, Fermi MI, Yuliausman, Elkardiana K, Sangaji AP, Ramadhan AM. The removal of dissolved ammonia from wastewater through a polypropylene hollow fiber membrane contactor. *Intl J Technol* 2015; 7: 1146-1152. <https://doi.org/10.14716/ijtech.v6i7.1845>
- [12] Lai C-L, Chen S-H, Liou R-M. Removing aqueous ammonia by membrane contactor process. *Desalination and Water Treatment* 2013; 51: 5307-5310. <https://doi.org/10.1080/19443994.2013.768788>

- [13] Norddahl B, Horn VG, Larsson M, du Preez JH, Christensen K. Desalination 2006; 199: 172-174.
<https://doi.org/10.1016/j.desal.2006.03.037>
- [14] Kartohardjono S, Herdiana M, Bismo S. Combination of ozonation and absorption through membrane contactor to remove ammonia from wastewater. Jurnal Teknik Indonesia 2012; 81-86.
- [15] Amaral MCS, Magalhaes NC, Moravia WG, Ferreira CD. Ammonia recovery from landfill leachate using hydrophobic membrane. Water Sci Technol 2016; 74: 2177-2184.
<https://doi.org/10.2166/wst.2016.375>

Received on 25-08-2018

Accepted on 18-02-2019

Published on 25-02-2019

DOI: <https://doi.org/10.6000/1929-6037.2019.08.01>